Computer Methods in Biomechanics and Biomedical Engineering
Vol. 12, No. 4, August 2009, 469–479

An analytical model for the ergometer rowing: inverse multibody dynamics analysis

L. Consiglieri[a]* and E.B. Pires[b]

[a]*Department of Mathematics and CMAF, Faculty of Sciences, University of Lisbon, 1749-016 Lisboa, Portugal;* [b]*Department of Civil Engineering and Architecture and ICIST, Instituto Superior Técnico, 1049-001 Lisboa, Portugal*

(*Received 26 September 2008; final version received 12 December 2008*)

Dedicated to our colleagues and friends A.B. Correia and J.A.C. Martins

A model for the ergometer rowing exercise is presented in this paper. From the quantitative observations of a particular trajectory (motion), the model is used to determine the moment of the forces produced by the muscles about each joint. These forces are evaluated according to the continuous system of equations of motion. An inverse dynamics analysis is performed in order to predict the joint torques developed by the muscles during the execution of the task. An elementary multibody mechanical system is used as an example to discuss the assumptions and procedures adopted.

Keywords: kinematic coordinates; Lagrange method; motion equations; torques; ergometer rowing

1. Introduction

In recent years, ergometer rowing has become a new competitive sport, a training for on-water race pace rowers or simply an indoor exercise for healthy purposes. This rowing motion is a continuous movement consisting of a stroke phase and a recovery phase, during which the rower glidingly returns to the initial position. To perform this movement, several factors contribute to minimise the energy (see Baudouin and Hawkins (2004) and the references therein). The main objective of this work is to provide a better understanding of the correlation between the human skeletal data, the initial position and the torques imposed on the joints. Then the necessary intra-muscular control can be identified.

The force generated by the biological system has been evaluated by the analysis of experimental data for the rowing exercise (see Pudlo et al. (2005) and the references therein). Non-invasive techniques cannot estimate the muscle forces accurately, and mathematical models are required to predict such forces. In spite of the uncertainty of the anthropometric and kinematic input data needed for the inverse dynamics procedure, due to inaccuracies of the testing equipment (see Riemer et al. (2008), Robert et al. (2007) and the references therein), it is essential that a correct model exists in order to evaluate the internal moments about the various body joints. Indeed, the development of computational methods in the last few decades produced a large impact in the assessment of theoretical models. The need for adoption of non-linear behaviours is also indisputable. Here a non-linear mathematical model is adopted, and dynamic descriptions and interpretations are presented for a simple performance of the referred activity. The Lagrangean method is applied to both 2D and 3D segment representations. The comparison with the classical Newton–Euler recursive procedure makes it possible to assess the simplicity of this method.

In this paper, a mathematical model defined by a system of ordinary differential equations (ODEs) is proposed and implemented. The aim is to study the coupled system of equations of motion describing body-segmental dynamics. To establish the best performance during ergometer rowing, it is important to collect all the corresponding data in order to determine the torques at the joints generated to maintain the movement.

In previous works an algorithm for a 2D inverse problem was presented (see Hahn et al. (2005), for instance). A simple 2D model for rowing seems to be adequate when the study is restricted to the performance of the legs in a planar configuration.

The equations of motion of the constrained biomechanical system are assembled using rigid bodies describing the anatomical segments interconnected by ideal joints. In our rigid segment assumptions, the shoulder and elbow joints have three rotational degrees of freedom, and the other joints are represented by hinges with one degree of freedom in flexion and extension in the sagittal plane. The movement is assumed to have a bilateral symmetry. The torso is not described by a unique rigid body but it is decomposed into the pelvis and the thorax, and care is taken of their interaction (the thoraco-lumbar angle). The pattern of extension/flexion of each joint is precisely studied. Kinematic data are acquired from the literature.

In the next section, the dynamical model characterised by the system of equations of motion is stated. Section 3

*Corresponding author. Email: lconsiglieri@gmail.com

ISSN 1025-5842 print/ISSN 1476-8259 online

DOI: 10.1080/10255840802687400
http://www.informaworld.com

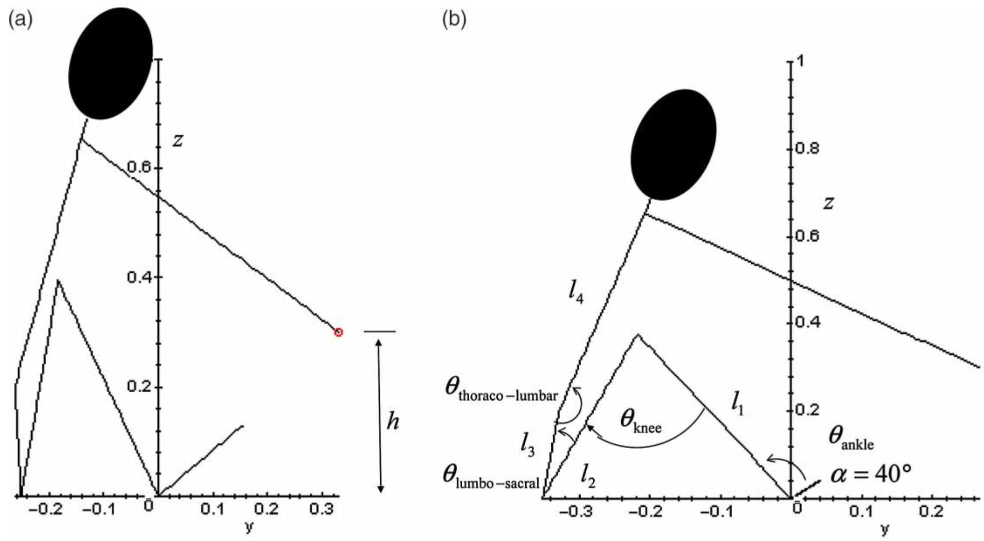

Figure 1. Schematic representations of the catch position.

presents and discusses the numerical results. The response of the model when some data are taken into account is then analysed. In Section 4 some conclusions are drawn and some open problems are listed. The ability of the model to evaluate the contribution of each torque joint is compared with the predictions. Finally, explicit formulas are presented in the Appendix.

2. Model

Ergometer rowing is a cyclic movement in which the subject pulls a handle that is connected to the flywheel that generates the rowing resistance. The rowing cycle is formed by the rower sliding back and forth along a monorail through the action of cyclical extension and flexion of the lower limbs. The propulsion phase begins at the catch position (i.e. full flexion of the lower limb and lumbar joints, and full extension of the upper limb joints, see Figure 1) and ends when the configuration characterised by full extension of the lower limb joints and full flexion of the upper limb joints is reached (see Figure 2). This phase is followed by

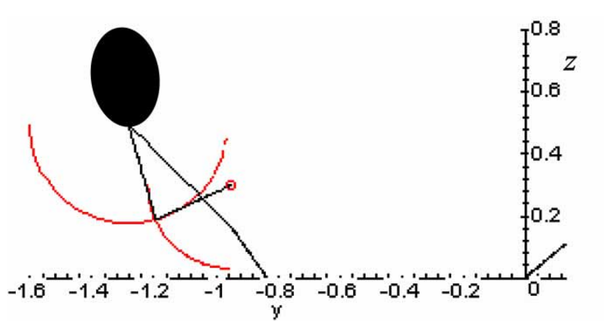

Figure 2. Schematic representation of the final position of the drive phase which coincides with the initial position of the recovery phase.

the return of the rower to the catch position of the next cycle, known as the recovery phase. It is assumed that the friction forces generated at the sliding seat during the rowing cycle are minimal, and are thus neglected.

The movement is formed by the trajectories of the joints in the Cartesian space. The human body model can be described by the feet at the cradle and by eight segments (the shank, the thigh, the pelvis, the head–trunk, the two upper arms and the two forearms including the hands). This 3D articulated linkage has its rigid body segments joined together by frictionless revolutes. The problem can be formulated, in matrix form, as

$$I(q)\ddot{q} = B(q, \dot{q}) + G(q) + T, \qquad (1)$$

where $q = (q_1, \ldots, q_8)$ are the generalised variables, $I(q)$ is the inertia mass matrix, $B(q, \dot{q})$ represents Coriolis and centrifugal effects, $G(q)$ gravitational and external effects and T the internal moments of force.

2.1 Kinematic equations

Since the exercise is symmetric at any instant of time $t > 0$, the movement can be considered to take place in the plane $0yz$, except for the set shoulder–elbow–wrist/hand (see Figure 3). However, the initial position of the human body, which corresponds to the beginning of the rowing exercise, can be completely described in the plane $0yz$ (Figure 1).

The origin of the 3D Cartesian reference frame is considered to be located at the ankle articulation (Figure 1(b)), and the position of each centre of mass is denoted by $(x_i,\ y_i,\ z_i)$ where $i = 1, \ldots, 6$ correspond, respectively, to the segments: (1) shank, (2) thigh, (3) pelvis, (4) head–trunk, (5) right upper arm and (6) right forearm–hand. The angles formed by the segments are

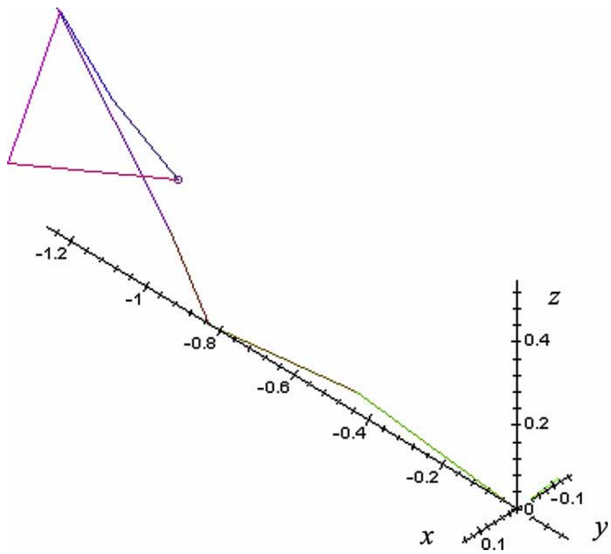

Figure 3. Schematic representation of an intermediate position.

denoted by θ_{ankle}, θ_{knee}, $\theta_{\text{lumbo-sacral}}$, $\theta_{\text{thoraco-lumbar}}$ and θ_{elbow} (see Figure 1). For each $i = 1, \ldots, 6$, m_i denotes the mass of segment i, r_i the distance between the centre of mass of each segment and the distal end and l_i the length of segment i from the distal to the proximal end. Notice that m_5 and m_6 are the masses of the two upper arms and forearms, respectively. Since the hand is closed, it is assumed to be without length. The centre of mass of the shank is given by

$$\begin{cases} x_1 = 0 \\ y_1 = r_1 \cos q_1 \\ z_1 = r_1 \sin q_1, \quad q_1 = \theta_{\text{ankle}} + \alpha, \end{cases}$$

where α is the fixed angle of the foot's support. The centre of mass of the thigh is given by

$$\begin{cases} x_2 = 0 \\ y_2 = l_1 \cos q_1 - r_2 \cos q_2 \\ z_2 = l_1 \sin q_1 - r_2 \sin q_2, \quad q_2 = \theta_{\text{ankle}} + \alpha - \theta_{\text{knee}}. \end{cases}$$

The seat position yields the following constraint which is introduced by the position of the hip at the horizontal level $z = 0$ and the fixed length of the thigh

$$l_1 \sin q_1 = l_2 \sin q_2,$$

and consequently

$$\cos q_2 = \sqrt{1 - \frac{l_1^2}{l_2^2} \sin^2 q_1}.$$

These conditions lower the problem's dimension by one unit, but the last equation poses some difficulties to the calculations. So q_2 will be kept as an unknown variable and only z_3 is simplified in the following kinematic equations of the centre of mass of the pelvis

$$\begin{cases} x_3 = 0 \\ y_3 = l_1 \cos q_1 - l_2 \cos q_2 + r_3 \cos q_3 \\ z_3 = r_3 \sin q_3, \quad q_3 = q_2 + \theta_{\text{lumbo-sacral}}. \end{cases}$$

Also z_4, in the kinematic equations of the centre of mass of the head–trunk, is taken as

$$\begin{cases} x_4 = 0 \\ y_4 = l_1 \cos q_1 - l_2 \cos q_2 + l_3 \cos q_3 + r_4 \cos q_4 \\ z_4 = l_3 \sin q_3 + r_4 \sin q_4, \quad q_4 = q_3 - 180^\circ + \theta_{\text{thoraco-lumbar}}. \end{cases}$$

The position (x_5, y_5, z_5) of the centre of mass of the right upper arm is given, as a function of the spherical coordinates q_5 and q_6, by

$$\begin{cases} x_5 = r_5 \sin q_5 \sin q_6 \\ y_5 = l_1 \cos q_1 - l_2 \cos q_2 + l_3 \cos q_3 + l_4 \cos q_4 + r_5 \sin q_5 \cos q_6 \\ z_5 = l_3 \sin q_3 + l_4 \sin q_4 - r_5 \cos q_5. \end{cases}$$

The centre of mass of the left upper arm is positioned at $(-x_5, y_5, z_5)$. The position (x_6, y_6, z_6) of the centre of mass of the right forearm is given, as a function of the spherical coordinates q_7 and q_8, by

$$\begin{cases} x_6 = l_5 \sin q_5 \sin q_6 + r_6 \sin q_7 \sin q_8 \\ y_6 = l_1 \cos q_1 - l_2 \cos q_2 + l_3 \cos q_3 + l_4 \cos q_4 + l_5 \sin q_5 \cos q_6 \\ \qquad + r_6 \sin q_7 \cos q_8 \\ z_6 = l_3 \sin q_3 + l_4 \sin q_4 - l_5 \cos q_5 - r_6 \cos q_7. \end{cases} \tag{2}$$

The centre of mass of the left forearm is positioned at $(-x_6, y_6, z_6)$.

If we consider $x_7 = 0$, so that the movement is correctly executed, the angles measured at the elbow between the two segments are known since the complex shoulder–elbow–wrist/hand is well defined by the angles q_5 and q_6, and the wrist–hand position $(0, y_7, z_7)$. Indeed the right forearm segment is also constrained by the position of the complex wrist–hand at the handle displacement $(0, y_7, z_7)$, i.e.

$$\begin{cases} x_6 = \left(1-\frac{r_6}{l_6}\right) l_5 \sin q_5 \sin q_6 \\ y_6 = \left(1-\frac{r_6}{l_6}\right)[l_1 \cos q_1 - l_2 \cos q_2 + l_3 \cos q_3 + l_4 \cos q_4 \\ \qquad\qquad + l_5 \sin q_5 \cos q_6] + \frac{r_6}{l_6} y_7 \\ z_6 = \left(1-\frac{r_6}{l_6}\right)[l_3 \sin q_3 + l_4 \sin q_4 - l_5 \cos q_5] + \frac{r_6}{l_6} z_7. \end{cases} \tag{3}$$

Moreover, the wrist–hand position at the handle displacement $(0, y_7, z_7)$ belongs to the spherical surface centered at the elbow articulation with radius l_6:

$$\begin{aligned} &(l_5 \sin q_5 \sin q_6)^2 + (l_1 \cos q_1 - l_2 \cos q_2 + l_3 \cos q_3 \\ &\quad + l_4 \cos q_4 + l_5 \sin q_5 \cos q_6 - y_7)^2 \\ &\quad + (l_3 \sin q_3 + l_4 \sin q_4 - l_5 \cos q_5 - z_7)^2 = l_6^2. \end{aligned}$$

Although this constraint also lowers another dimension to the problem, q_7 and q_8 are kept as unknown variables in order to simplify the calculations.

2.2 Motion equations

The equations of motion can be derived by means of the Lagrange method. With $q = (q_1, \ldots, q_8)$ and (x_i, y_i, z_i) as above, consider the Lagrangean operator

$$\begin{aligned} L(q_1, \ldots, q_8) = &\sum_{i=1}^{6} \left(\frac{1}{2} m_i \left((\dot{x}_i)^2 + (\dot{y}_i)^2 + (\dot{z}_i)^2 \right) - m_i g z_i \right) \\ &+ \sum_{j=1}^{8} I_j (\dot{q}_j)^2, \end{aligned}$$

representing the algebraic sum of the kinetic and the potential energies. The problem is defined by the equations $(k = 1, \ldots, 8)$

$$\frac{d}{\mathrm{d}t}\left(\frac{\partial L}{\partial \dot{q}_k}\right) - \frac{\partial L}{\partial q_k} = F_k \tag{4}$$

with

$$F = \begin{bmatrix} T_1 - T_2 \\ T_2 - T_3 - (l_2 \cos q_2 - l_1 \cos q_1) F_{\mathrm{seat}} \\ T_3 - T_4 + (l_2 \cos q_2 - l_1 \cos q_1) F_{\mathrm{seat}} \\ T_4 - T_5 \\ T_5 - T_7 \\ T_6 - T_8 \\ T_7 + y_7 F_{7z} - z_7 F_{7y} \\ T_8 \end{bmatrix}$$

where each T_k denotes the kth joint torque in the x-direction $(k = 1, \ldots, 5)$, T_6 the fifth joint torque in the z-direction, and T_7 and T_8 the sixth joint torque in the x- and z-directions, respectively, which are assumed constant and independent of the angular displacement of the joint. The vector $(0, 0, F_{\mathrm{seat}})$ denotes the vertical force applied by the sliding seat on the rower ischia, and $F_{\mathrm{handle}} = (0, F_{7y}, F_{7z})$ represents the external force generated by the flywheel's mechanism and the air resistance transmitted to the two hands. Note that the moment of the reaction force at the foot cradle, $F_{\mathrm{stretcher}} = (0, F_{1y}, F_{1z})$, vanishes because this force is located at the origin of the coordinate system.

Indeed, rewriting the Lagrangean operator as

$$L(q_1, \ldots, q_8) = \frac{1}{2} \sum_{i,j=1}^{8} \dot{q}_i I_{ij}(q) \dot{q}_j - g \sum_{i=1}^{6} m_i z_i(q),$$

and observing that the inertia mass matrix I is symmetric, it is possible to obtain (1) from (4) providing that

$$B(q, \dot{q}) = -\left[\sum_{i,j=1}^{8} \dot{q}_i \left(\frac{\partial I_{ik}}{\partial q_j} - \frac{1}{2} \frac{\partial I_{ij}}{\partial q_k} \right) \dot{q}_j \right]_{k=1,\ldots,8}$$

$$C(q) = -\left[\sum_{i=1}^{6} m_i g \frac{\partial z_i}{\partial q_k} \right]_{k=1,\ldots,8}$$

$$G(q) = C(q) + \begin{bmatrix} 0 \\ -(l_2 \cos q_2 - l_1 \cos q_1) F_{\mathrm{seat}} \\ (l_2 \cos q_2 - l_1 \cos q_1) F_{\mathrm{seat}} \\ 0 \\ 0 \\ 0 \\ y_7 F_{7z} - z_7 F_{7y} \\ 0 \end{bmatrix}.$$

Explicit expressions are given in the Appendix.

Then the inverse multibody dynamics analysis can be stated as

$$\begin{bmatrix} T_1 \\ T_2 \\ \vdots \\ T_8 \end{bmatrix} = \begin{bmatrix} 1 & 1 & \ldots & 1 & 0 & 1 & 0 \\ 0 & 1 & \ldots & 1 & 0 & 1 & 0 \\ \vdots & \ddots & \ddots & \vdots & \vdots & \vdots & \vdots \\ 0 & 0 & \ddots & 1 & 0 & 1 & 0 \\ 0 & 0 & \ldots & 0 & 1 & 0 & 1 \\ 0 & 0 & \ldots & 0 & 0 & 1 & 0 \\ 0 & 0 & \ldots & 0 & 0 & 0 & 1 \end{bmatrix} \cdot \left(I(q)\ddot{q} - B(q, \dot{q}) - G(q) \right). \tag{5}$$

Table 1. Body segment parameters (McConville et al. 1980).

	Shank ($i = 1$)	Thigh ($i = 2$)	Pelvis ($i = 3$)	Head–trunk ($i = 4$)
m_i (kg)	7.5	15.2	10.5	31.3
r_i (m)	0.274	0.251	0.1	0.143
l_i (m)	0.435	0.4	0.2	0.475
I_i (kg m)	0.065	0.126	0.08	1.39

Table 2. Upper limbs segment parameters (McConville et al. 1980).

	Upper arm ($i = 5$)	Forearm–hand ($i = 6$)
m_i (kg)	3.5	2.3
r_i (m)	0.15	0.12
l_i (m)	0.33	0.27
I_{xx} (kg m)	$I_5 = 0.01$	$I_7 = 0.006$
I_{zz}	$I_6 = 0.01$	$I_8 = 0.006$

3. Results

This section is divided into theoretical and numerical results.

3.1 *Theoretical results*

At the initial drive phase (0–20%), both the upper limbs are fully extended ($\theta_{\text{elbow}} = 180°$) and located at the sagittal plane ($q_6 = 0$), i.e. $x = 0$. Thus it follows that

$$(l_5 + l_6)^2 = (Y_4(t) - y_7(t))^2 + (Z_4(t) - z_7(t))^2, \qquad (6)$$

where (0, Y_4, Z_4) denotes the 3D-position of the shoulder articulation:

$$\begin{cases} Y_4 = l_1 \cos q_1 - l_2 \cos q_2 + l_3 \cos q_3 + l_4 \cos q_4 \\ Z_4 = l_3 \sin q_3 + l_4 \sin q_4. \end{cases} \qquad (7)$$

Note that, at the initial instant, the position of the complex wrist–hand is known

$$\begin{cases} x_7(0) = 0.0 \\ y_7(0) = l_1 \cos q_1(0) - l_2 \cos q_2(0) + l_3 \cos q_3(0) \\ \qquad\qquad + l_4 \cos q_4(0) + (l_5 + l_6) \sin q_5(0) \\ z_7(0) = l_3 \sin q_3(0) + l_4 \sin q_4(0) - (l_5 + l_6) \cos q_5(0) \end{cases}$$

which coincides with the initial position $(x_7, y_7, z_7)(0) = (0, y_7(0), h)$, where $h = z_7(0)$. During the rowing cycle, the vertical coordinate of the wrist–hand complex should remain constant and equal to h for the exercise to be correctly performed. Consequently the upper limbs should satisfy the constraints

$$q_5(t) = \arccos\left(\frac{Z_4(t) - h}{l_5 + l_6}\right); \qquad (8)$$

$$y_7(t) = Y_4(t) + \sqrt{(l_5 + l_6)^2 - (Z_4(t) - h)^2}. \qquad (9)$$

At the final instant of the drive stage, i.e. at the final instant of the stroke phase ($t = 40\%$), both the upper limbs are assumed to be in the sagittal plane ($x = 0$) and the following constraint arises

$$y_7(t) \geq -l_1 - l_2 + l_3 \cos q_3(t) + (h - l_3 \sin q_3(t))/\tan(q_4(t)).$$

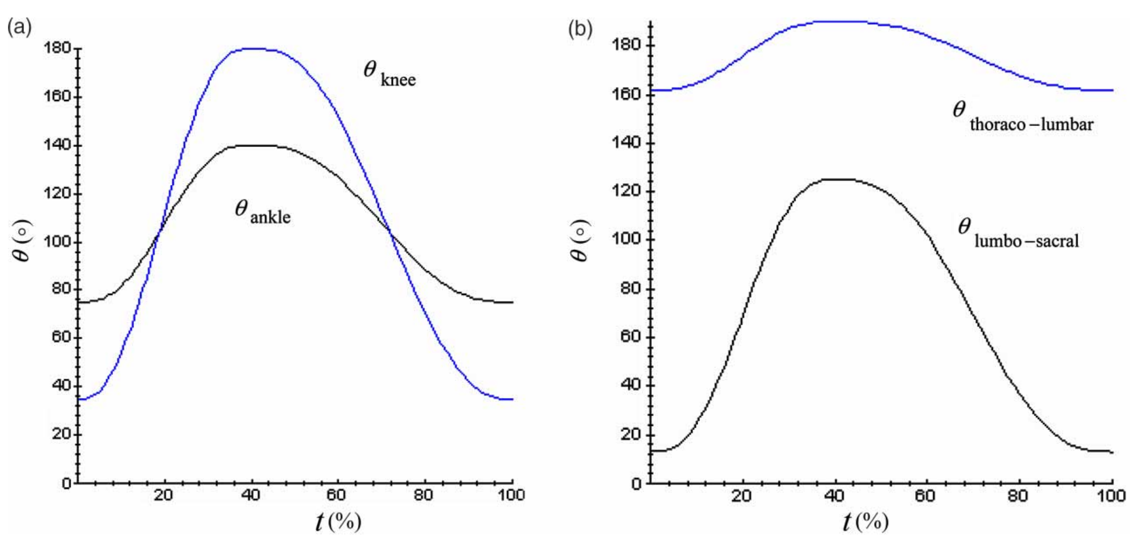

Figure 4. Example of phasic angular displacement patterns normalised in time as percentage of the cycle of the ergometer rowing. (a) Lower limbs: ankle angle $\theta_{\text{ankle}} = q_1 - \alpha$ and knee angle $\theta_{\text{knee}} = q_1 - q_2$. (b) Trunk: lumbo-sacral angle $\theta_{\text{lumbo–sacral}} = q_3 - q_2$, and thoraco-lumbar angle $\theta_{\text{thoraco–lumbar}} = q_4 - q_3 + 180°$.

This inequality means that at the instant $t = 40\%$ the handle is at most positioned at the rower's torso.

Moreover, from the human body constraints (2)–(3), it is possible to obtain explicit expressions for the elbow angles. More precisely, it follows from (2)–(3) that

$$q_7 = \arccos\left(\frac{1}{l_6}(l_3\sin q_3 + l_4\sin q_4 - l_5\cos q_5 - h)\right),$$
$$q_8 = \arcsin\left(-\frac{l_5\sin q_5\sin q_6}{l_6\sin q_7}\right).$$

Once the elbow angle θ_{elbow} is known it is possible to calculate y_7.

Finally, from Equations (2)–(3) it follows that

$$\begin{cases} (l_6 \sin q_7 \sin q_8)^2 = (-l_5 \sin q_5 \sin q_6)^2 \\ (l_6 \sin q_7 \cos q_8)^2 = (-l_5 \sin q_5 \cos q_6 - (Y_4 - y_7))^2 \end{cases}$$

and summing, it results that

$$(l_6\sin q_7)^2 = (l_5\sin q_5)^2 + 2l_5(Y_4 - y_7)\sin q_5\cos q_6 + (Y_4 - y_7)^2.$$

Then, we conclude that

$$q_6 = \arccos\left(\frac{(l_6\sin q_7)^2 - (l_5\sin q_5)^2 - (Y_4 - y_7)^2}{2l_5(Y_4 - y_7)\sin q_5}\right).$$

3.2 Numerical results

In this section, numerical results of the system (5) are presented for the two different initial conditions of the handle position:

$$A:\ y_7(0) = 0.2,\ h = 0.17 \quad \text{and} \quad B:\ y_7(0) = 0.33,\ h = 0.3.$$

In Tables 1 and 2 the data parameters for a subject with weight 70 kg and height 1.70 m are listed. Notice that neither the weight of the feet, because they do not interfere in the rowing movement, nor the height of the complex neck–head are considered.

Figure 4 shows the profiles of θ_{ankle} and θ_{knee} performed by the lower limbs, and the profiles of $\theta_{\text{lumbo-sacral}}$ and $\theta_{\text{thoraco-lumbar}}$ performed by the trunk (adapted from Bull and McGregor (2000)). Figure 5 displays the profile of the elbow angle θ_{elbow} for the two cases A and B. Under the constraints stated in Section 3.1, it is possible to obtain the profiles of y_7 (Figure 6) and of the spherical coordinates q_6, q_7 and q_8 (Figure 7). Notice that q_5 has the explicit formula (8) at the initial drive phase (0–20%). Indeed, q_5 is given if q_6, q_7 and q_8 are considered constrained.

The sliding seat load has a bell shape (see Figure 8, adapted from Colloud et al. (2006)), reaching its maximum when the lower limbs and trunk are fully extended.

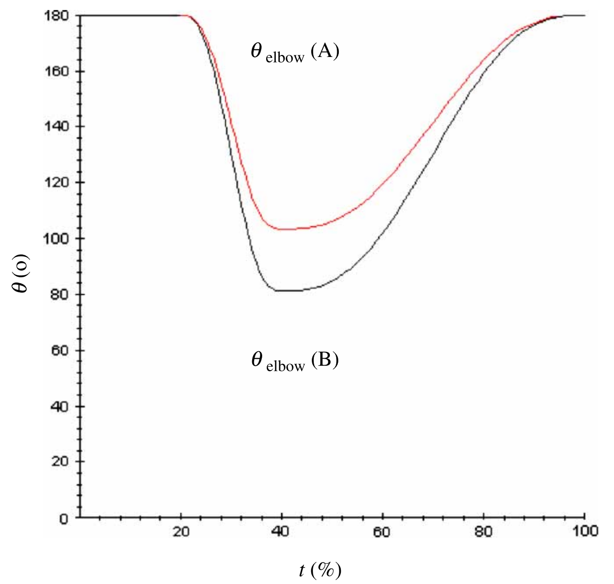

Figure 5. Elbow angle profile (θ_{elbow}), while the A- and B-cycles of the ergometer rowing are performed during the time duration (0–100%).

The anterior–posterior handle force has a bell-shaped profile (see Figure 9, adapted from Colloud et al. (2006)) with a rapid increase in the magnitude of the force until a peak is reached, followed by a decrease. After this decrease a constant value is reached, which is found to be equal to the traction force provided by the elasticity of the self-recoiling system. The vertical handle force also shows a reverse bell shape in the propulsion phase (see Figure 9, adapted from Colloud et al. (2006)).

The contribution of each joint torque to the action of the muscles is obtained from the calculation of the whole system of ODEs (5). Figure 10 shows the profiles in the

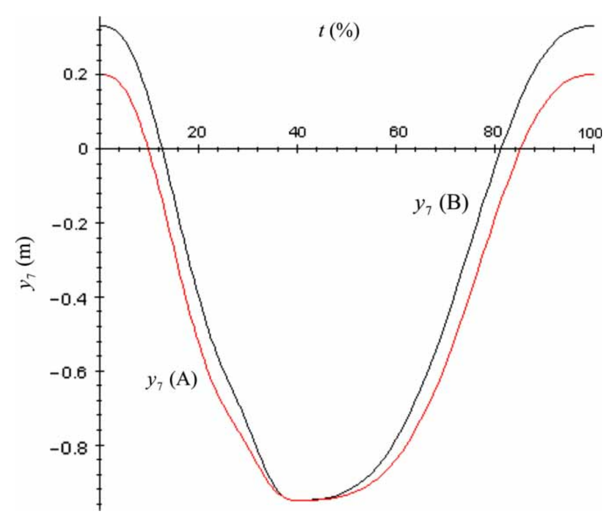

Figure 6. Antero-posterior handle displacement (y_7), while the A- and B-cycles of the ergometer rowing are performed during the time duration (0–100%).

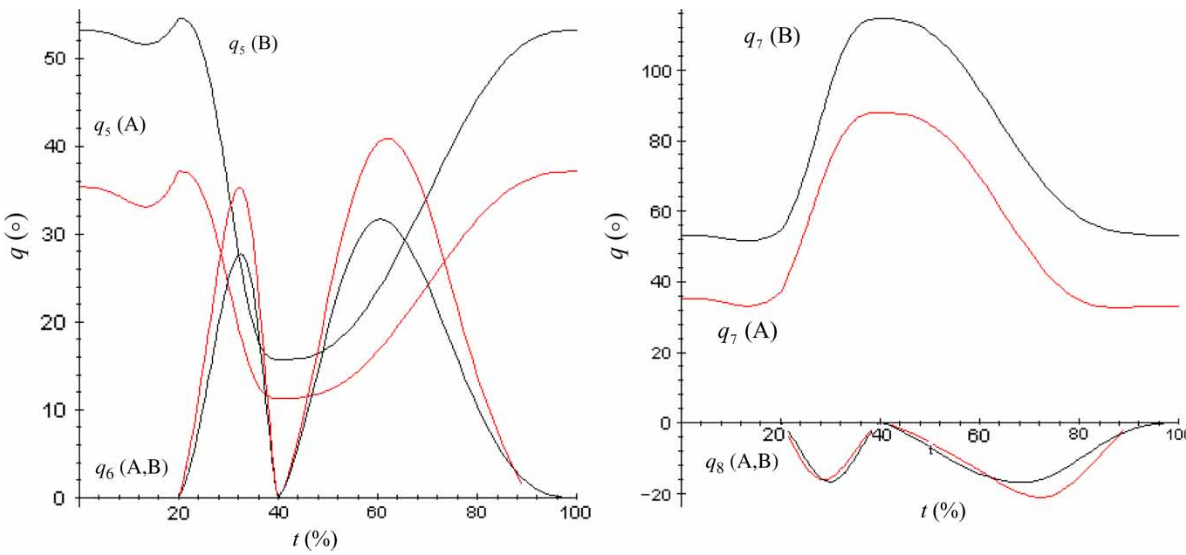

Figure 7. Spherical coordinates q_5 and q_6 for the shoulder and q_7 and q_8 for the elbow, while the A- and B-cycles of the ergometer rowing are performed.

z-direction of the torques, T_8 (about the elbow joint) and T_6 (about the shoulder joint), corresponding to the B-cycle, which practically coincide with the profiles for the other cycle (A). The remaining torques in the x-direction are shown in Figure 11 (A-cycle), Figure 12 (B-cycle) and Figure 13 (both cycles).

4. Conclusions and open problems

In this paper, the full cycle for the exercise in a rowing ergometer was reconstructed by assuming bilateral symmetry. The initial antero-posterior position y_7 of the handle relative to the stretcher in the reference frame is slightly positive at the catch because the handle was located ahead of the stretcher (see Figures 1 and 6). At the first phase (0–20%) the rower cycle is performed at the sagittal plane ($q_8 = q_6 = 0$) with the upper limbs fully extended ($\theta_{\text{elbow}} = 180°$, cf. Figure 5). Then $T_8 = T_6 = 0$ as expected. No significant values in magnitude are revealed in the remaining patterns of T_6 and T_8, although the existence of a peak for the shoulder joint torque T_6 in the z-direction, at the final instant of the stroke phase ($t = 40\%$), is consistent with the position of the upper arm in relation to the torso. The profiles obtained for the torques are as predicted: the maximum and minimum values occur at the same instants as the peaks of the external forces. Indeed, for the joints of the upper body, the peaks

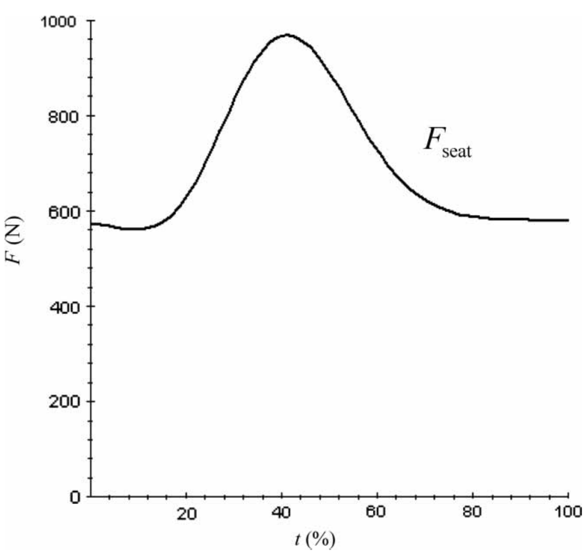

Figure 8. Vertical seat force (F_{seat}) as a function of percentage of time.

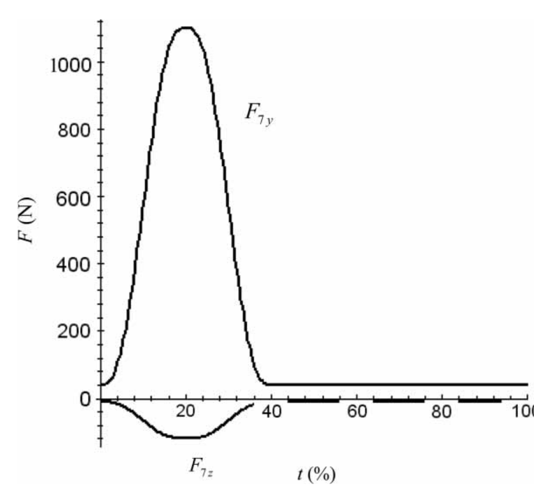

Figure 9. Antero-posterior and vertical handle forces (F_{7y} and F_{7z}, respectively) as functions of percentage of time. A negative value indicates that the body is pushing backwards (F_{7y}) or downwards (F_{7z}) during the driving phase.

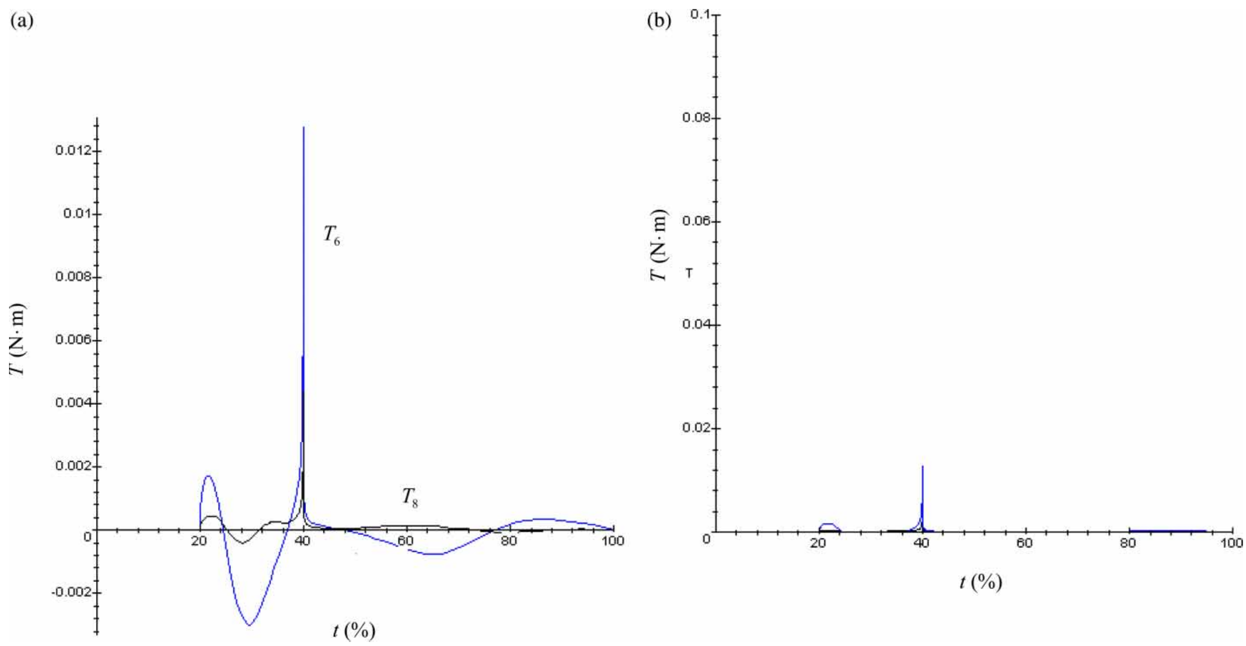

Figure 10. The joint torques T_6 and T_8 corresponding to the shoulder and elbow joints in the z-direction, under different scales (a) <0.013 N m and (b) <0.1 N m.

of T_4, T_5 and T_7 match the ones of the handle forces (see Figure 9). The activity of T_5 and T_7 ends when the drive phase finishes. In the recovery phase, T_5 and T_7 show no significant activity. The profiles of T_1, T_2 and T_3, corresponding to the joints of the lower extremity, have their maximum in accordance with the peaks of the handle forces at the propulsion phase and have their minimum in accordance with the peak of the seat force at the remaining drive and recovery phases.

These results are consistent with the muscle activity patterns of experienced rowers on the Concept 2C (cf. Nowicky et al. 2005), and they support the hypothesis of a minimum-metabolic-energy in rowing.

The agreement between the torques for the A- and B-cycles is also as expected. The relevant differences are: (1) the maximum values obtained for T_4, T_5 and T_7, (A-cycle: $\simeq 150$ N m, B-cycle: $\simeq 300$ N m); and (2) the profiles of T_1, T_2 and T_3 differ at the initial phase. These variations reflect

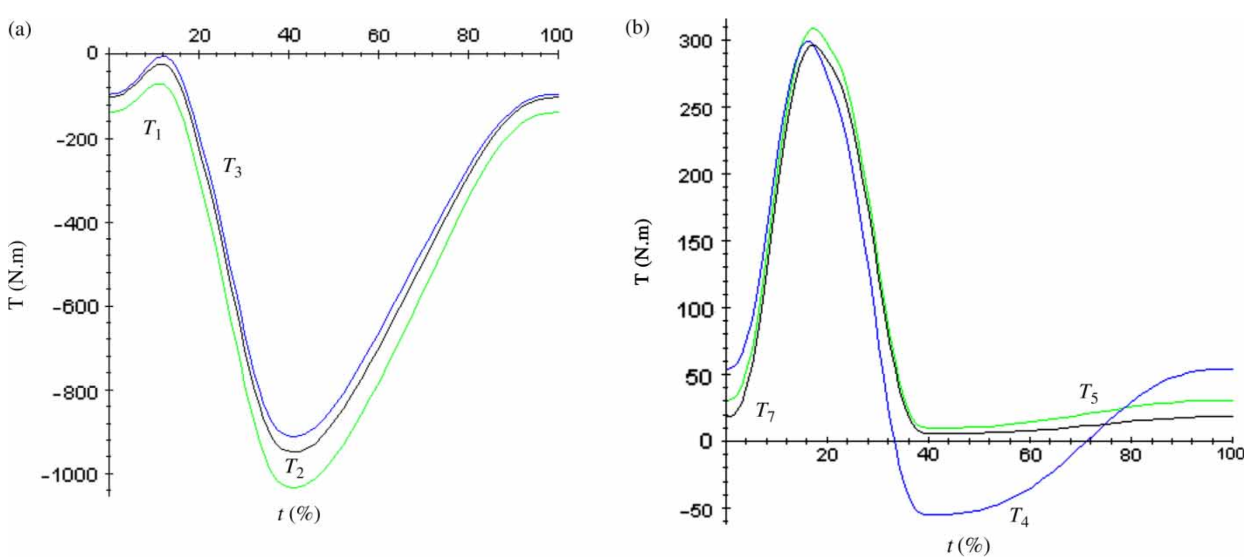

Figure 11. The joint torques in the x-direction while the A-cycle of the ergometer rowing is performed during the time duration (0–100%). (a) The joint torques T_1, T_2 and T_3 corresponding to the ankle, knee and lower torso, respectively. (b) The torques T_4, T_5 and T_7 corresponding to the lumbar, shoulder and elbow joints, respectively.

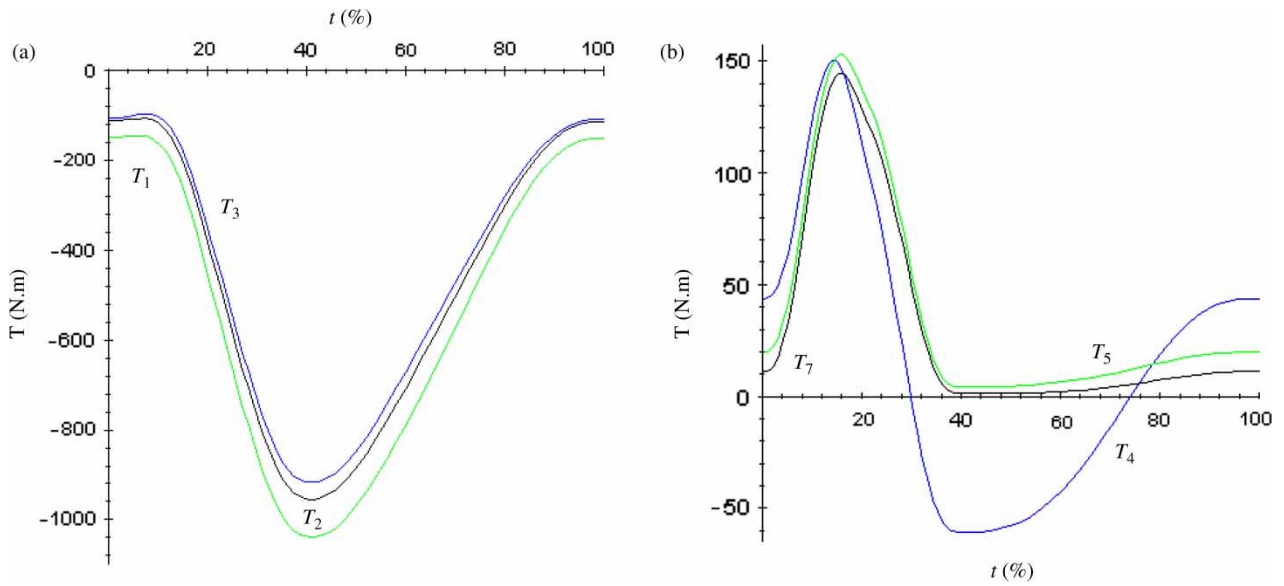

Figure 12. The joint torques in the x-direction while the B-cycle of the ergometer rowing is performed. (a) The joint torques T_1, T_2 and T_3 corresponding to the ankle, knee and lower torso, respectively. (b) The torques T_4, T_5 and T_7 corresponding to the lumbar, shoulder and elbow joints, respectively.

the fact that the activity of the moments of force is lower in the A-cycle than in the B-cycle which is consistent with the initial positions $y_7(0) = 0.2$ and $y_7(0) = 0.33$, respectively. In conclusion, an appropriate initial position of the upper limbs decreases the risk factors for injuries.

A statistical analysis describing the motion and load characteristics of ergometer rowing is used to test the hypothesis that the rowing stroke technique is associated with the incidence of low back pain (see O'Sullivan et al. (2003)). Indeed, the use of the values obtained for the torques may improve the performance and prevent injuries such as back pain.

The present theoretical model was numerically examined by solving the two examples (cf. Section 3.2), but it can be applied to a large number of rower's performances since the assumptions considered correspond to the exercise in a rowing ergometer (cf. Section 2.1). For instance, the seat slides along the central bar or the two hands of the rower grasp the handle that is attached by a chain to the flywheel which in turn puts a fan in motion. Only the bilateral symmetry of the rowing movement and the correctness of the horizontal trajectory of the handle were assumed in order to simplify the presentation. Also the data taken from the literature have these same characteristics corresponding

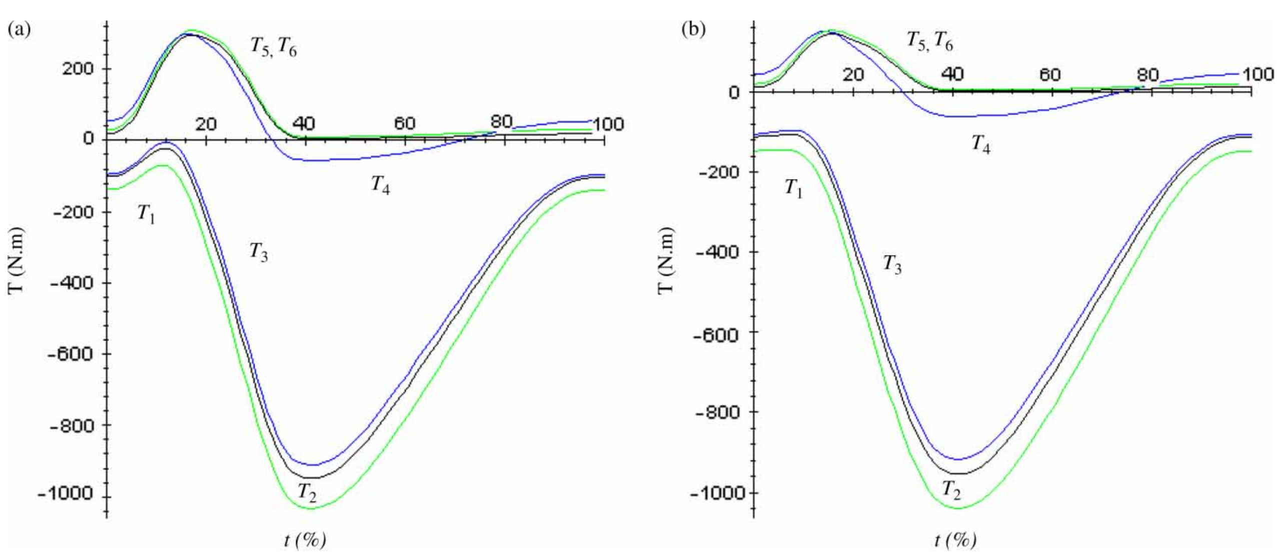

Figure 13. The joint torques in the x-direction during the time duration (0–100%). (a) The joint torques T_1, T_2, T_3, T_4, T_5 and T_7 for the A-cycle. (b) The torques T_1, T_2, T_3, T_4, T_5 and T_7 for the B-cycle.

to the stable base of the ergometer. Notice that these two limitations can be removed with the obvious implication of having to deal with a more complex model. Future work should exclude these two limitations in order to provide a complete study on the relation between involuntary inaccurate movements and lumbar pains (see Pudlo et al. (2005) and the references therein). Moreover, a 3D asymmetric model may be applied to rowing in water, in which the oarsman is subjected to different loads.

To study the contribution of the joint torques in human movements it is imperative that accurate mathematical models (see Consiglieri and Pires (2007), for instance) exist. We believe that the ability to predict internal moments is particularly important because it offers the possibility of investigating the impacts of the coordination and function of the movements on the human structure. The results obtained with different sets of data can lead to improvements in the procedures for the correction of joint performances and in the prevention of injuries.

References

Baudouin A, Hawkins D. 2004. Investigation of biomechanical factors affecting rowing performance. J Biomech. 37(7): 969–976.

Bull AMJ, McGregor AH. 2000. Measuring spinal motion in rowers: the use of an electromagnetic device. Clin Biomech. 15(10):772–776.

Colloud F, Bahuaud P, Doriot N, Champely S, Chèze L. 2006. Fixed versus free-floating stretcher mechanism in rowing ergometers: mechanical aspects. J Sports Sci. 24(5): 479–493.

Consiglieri L, Pires EB. 2007. Analytical approach for the evaluation of the torques using inverse multibody dynamics. Multibody Syst Dyn. 18(3):471–483.

Hahn D, Schwirtz A, Huber A. 2005. Anthropometric standardisation of multiarticular leg extension movements: a theoretical study. Isokinet Exerc Sci. 13(2):95–101.

McConville JT, Clauser CE, Churchill TD, Cuzzi J, Kaleps I. 1980. Anthropometric relationships of body and body segment moments of inertia. In: Technical Report AFAMRL-TR-80-119. Wright-Patterson AFB, OH: Air Force Aerospace Medical Research Laboratory.

Nowicky AV, Burdett R, Horne S. 2005. The impact of ergometer design on hip and trunk muscle activity patterns in elite rowers: an electromyographic assessment. J Sports Sci Med. 4(1):18–28.

O'Sullivan F, O'Sullivan J, Bull AMJ, McGregor AH. 2003. Modelling multivariate biomechanical measurements of the spine during a rowing exercise. Clin Biomech. 18(6):488–493.

Pudlo P, Pinti A, Lepoutre FX. 2005. Experimental laboratory apparatus to analyze kinematics and 3D kinetics in rowing. Sports Eng. 8(1):39–46.

Riemer R, Hsiao-Wecksler ET, Zhang X. 2008. Uncertainties in inverse dynamics solutions: a comprehensive analysis and an application to gait. Gait Posture. 27(4):578–588.

Robert T, Chèze L, Dumas R, Verriest J-P. 2007. Validation of net joint loads calculated by inverse dynamics in case of complex movements: application to balance recovery movements. J Biomech. 40(11):2450–2456.

Appendix

The coefficients of the symmetric inertia matrix I in Equation (1) are:

$$
\begin{aligned}
I_{11} &= I_1 + m_1 r_1^2 + m_2 l_1^2 + (m_3+m_4+m_5+m_6) l_1^2 \sin^2 q_1 \\
I_{12} &= -m_2 l_1 r_2 \cos(q_1 - q_2) \\
&\quad - (m_3+m_4+m_5+m_6) l_1 l_2 \sin q_1 \sin q_2 \\
I_{13} &= c_3 l_1 \sin q_1 \sin q_3 \\
I_{14} &= c_4 l_1 \sin q_1 \sin q_4 \\
I_{15} &= -c_5 l_1 \sin q_1 \cos q_5 \cos q_6 \\
I_{16} &= c_5 l_1 \sin q_1 \sin q_5 \sin q_6 \\
I_{17} &= -c_6 l_1 \sin q_1 \cos q_7 \cos q_8 \\
I_{18} &= c_6 l_1 \sin q_1 \sin q_7 \sin q_8 \\
I_{22} &= I_2 + m_2 r_2^2 + (m_3+m_4+m_5+m_6) l_2^2 \sin^2 q_2 \\
I_{23} &= -c_3 l_2 \sin q_2 \sin q_3 \\
I_{24} &= -c_4 l_2 \sin q_2 \sin q_4 \\
I_{25} &= c_5 l_2 \sin q_2 \cos q_5 \cos q_6 \\
I_{26} &= -c_5 l_2 \sin q_2 \sin q_5 \sin q_6 \\
I_{27} &= c_6 l_2 \sin q_2 \cos q_7 \cos q_8 \\
I_{28} &= -c_6 l_2 \sin q_2 \sin q_7 \sin q_8 \\
I_{33} &= I_3 + m_3 r_3^2 + (m_4+m_5+m_6) l_3^2 \\
I_{34} &= c_4 l_3 \cos(q_3 - q_4) \\
I_{35} &= c_5 l_3 (\cos q_3 \sin q_5 - \sin q_3 \cos q_5 \cos q_6) \\
I_{36} &= c_5 l_3 \sin q_3 \sin q_5 \sin q_6 \\
I_{37} &= c_6 l_3 (\cos q_3 \sin q_7 - \sin q_3 \cos q_7 \cos q_8) \\
I_{38} &= c_6 l_3 \sin q_3 \sin q_7 \sin q_8 \\
I_{44} &= I_4 + m_4 r_4^2 + (m_5+m_6) l_4^2 \\
I_{45} &= c_5 l_4 (\cos q_4 \sin q_5 - \sin q_4 \cos q_5 \cos q_6) \\
I_{46} &= c_5 l_4 \sin q_4 \sin q_5 \sin q_6 \\
I_{47} &= c_6 l_4 (\cos q_4 \sin q_7 - \sin q_4 \cos q_7 \cos q_8) \\
I_{48} &= c_6 l_4 \sin q_4 \sin q_7 \sin q_8 \\
I_{55} &= I_5 + m_5 r_5^2 + m_6 l_5^2 \\
I_{56} &= 0 \\
I_{57} &= c_6 l_5 (\cos q_5 \cos q_7 \cos(q_6 - q_8) + \sin q_5 \sin q_7) \\
I_{58} &= c_6 l_5 \cos q_5 \sin q_7 \sin(q_6 - q_8) \\
I_{66} &= I_6 + \left(m_5 r_5^2 + m_6 l_5^2\right) \sin^2 q_5 \\
I_{67} &= c_6 l_5 \sin q_5 \cos q_7 \sin(q_8 - q_6) \\
I_{68} &= c_6 l_5 \sin q_5 \sin q_7 \cos(q_8 - q_6) \\
I_{77} &= I_7 + m_6 r_6^2 \\
I_{78} &= 0 \\
I_{88} &= I_8 + m_6 r_6^2 \sin^2 q_7
\end{aligned}
$$

where

$$
\begin{aligned}
c_3 &= m_3 r_3 + (m_4+m_5+m_6) l_3 \\
c_4 &= m_4 r_4 + (m_5+m_6) l_4 \\
c_5 &= m_5 r_5 + m_6 l_5 \\
c_6 &= m_6 r_6.
\end{aligned}
$$

The (8 × 1) Coriolis matrix takes the form

$$B(q,\dot q) = \begin{bmatrix} B_{11} & \dots & B_{19} & B_{10} \\ \vdots & & \vdots & \vdots \\ B_{81} & \dots & B_{89} & B_{80} \end{bmatrix}_{(8\times 10)} \begin{bmatrix} \dot q_1^2 \\ \vdots \\ \dot q_8^2 \\ \dot q_5 \dot q_6 \\ \dot q_7 \dot q_8 \end{bmatrix}$$

where

$$B_{33} = B_{44} = B_{55} = B_{59} = B_{65} = B_{66} = B_{77} = B_{70} = B_{87} = B_{88} = B_{80} = 0,$$

$$B_{11} = -\frac{1}{2}\frac{\partial I_{11}}{\partial q_1} = -(m_3+m_4+m_5+m_6)l_1^2 \sin q_1 \cos q_1$$

$$B_{12} = -\frac{\partial I_{12}}{\partial q_2} = m_2 l_1 r_2 \sin(q_1 - q_2) + (m_3+m_4+m_5+m_6)l_1 l_2 \sin q_1 \cos q_2$$

$$B_{1j} = -\frac{\partial I_{1j}}{\partial q_j} = -c_j l_1 \sin q_1 \cos q_j, \quad j = 3,4$$

$$B_{15} = B_{16} = -\frac{\partial I_{1j}}{\partial q_j} = -c_5 l_1 \sin q_1 \sin q_5 \cos q_6, \quad j = 5,6$$

$$B_{17} = B_{18} = -\frac{\partial I_{1j}}{\partial q_j} = -c_6 l_1 \sin q_1 \sin q_7 \cos q_8, \quad j = 7,8$$

$$B_{19} = -\left(\frac{\partial I_{15}}{\partial q_6} + \frac{\partial I_{16}}{\partial q_5}\right) = -2c_5 l_1 \sin q_1 \cos q_5 \sin q_6,$$

$$B_{10} = -2c_6 l_1 \sin q_1 \cos q_7 \sin q_8,$$

$$B_{21} = -\frac{\partial I_{21}}{\partial q_1} = m_2 l_1 r_2 \sin(q_2 - q_1) + (m_3+m_4+m_5+m_6)l_1 l_2 \cos q_1 \sin q_2$$

$$B_{22} = -\frac{1}{2}\frac{\partial I_{22}}{\partial q_2} = -(m_3+m_4+m_5+m_6)l_2^2 \sin q_2 \cos q_2$$

$$B_{2j} = -\frac{\partial I_{2j}}{\partial q_j} = c_j l_2 \sin q_2 \cos q_j, \quad j = 3,4$$

$$B_{25} = B_{26} = -\frac{\partial I_{2j}}{\partial q_j} = c_5 l_2 \sin q_2 \sin q_5 \cos q_6, \quad j = 5,6$$

$$B_{27} = B_{28} = -\frac{\partial I_{2j}}{\partial q_j} = c_6 l_2 \sin q_2 \sin q_7 \cos q_8, \quad j = 7,8$$

$$B_{29} = -\left(\frac{\partial I_{25}}{\partial q_6} + \frac{\partial I_{26}}{\partial q_5}\right) = 2c_5 l_2 \sin q_2 \cos q_5 \sin q_6,$$

$$B_{20} = 2c_6 l_2 \sin q_2 \cos q_7 \sin q_8,$$

$$B_{i1} = -c_i l_1 \cos q_1 \sin q_i, \quad i = 3,4$$

$$B_{i2} = c_i l_2 \cos q_2 \sin q_i, \quad i = 3,4$$

$$B_{34} = -\frac{\partial I_{34}}{\partial q_4} = c_4 l_3 \sin(q_4 - q_3)$$

$$B_{i5} = -c_5 l_i (\cos q_i \cos q_5 + \sin q_i \sin q_5 \cos q_6), \quad i = 3,4$$

$$B_{i6} = -c_5 l_i \sin q_i \sin q_5 \cos q_6, \quad i = 3,4$$

$$B_{i7} = -c_6 l_i (\cos q_i \cos q_7 + \sin q_i \sin q_7 \cos q_8), \quad i = 3,4$$

$$B_{i8} = -c_6 l_i \sin q_i \sin q_7 \cos q_8, \quad i = 3,4$$

$$B_{i9} = -2c_5 l_i \sin q_i \cos q_5 \sin q_6, \quad i = 3,4$$

$$B_{i0} = -2c_6 l_i \sin q_i \cos q_7 \sin q_8, \quad i = 3,4$$

$$B_{43} = -\frac{\partial I_{43}}{\partial q_3} = c_4 l_3 \sin(q_3 - q_4)$$

$$B_{51} = -\frac{\partial I_{51}}{\partial q_1} = c_5 l_1 \cos q_1 \cos q_5 \cos q_6$$

$$B_{52} = -\frac{\partial I_{52}}{\partial q_2} = -c_5 l_2 \cos q_2 \cos q_5 \cos q_6$$

$$B_{5j} = c_5 l_j (\sin q_j \sin q_5 + \cos q_j \cos q_5 \cos q_6), \quad j = 3,4$$

$$B_{56} = -\left(\frac{\partial I_{65}}{\partial q_6} - \frac{1}{2}\frac{\partial I_{66}}{\partial q_5}\right) = \left(m_5 r_5^2 + m_6 l_5^2\right)\sin q_5 \cos q_5$$

$$B_{57} = -\frac{\partial I_{57}}{\partial q_7} = -c_6 l_5 (-\cos q_5 \sin q_7 \cos(q_6 - q_8) + \sin q_5 \cos q_7)$$

$$B_{58} = c_6 l_5 \cos q_5 \sin q_7 \cos(q_6 - q_8),$$

$$B_{50} = 2c_6 l_5 \cos q_5 \cos q_7 \sin(q_8 - q_6),$$

$$B_{61} = -c_5 l_1 \cos q_1 \sin q_5 \sin q_6$$

$$B_{62} = c_5 l_2 \cos q_2 \sin q_5 \sin q_6$$

$$B_{6j} = -c_5 l_j \cos q_j \sin q_5 \sin q_6, \quad j = 3,4$$

$$B_{67} = B_{68} = c_6 l_5 \sin q_5 \sin q_7 \sin(q_8 - q_6),$$

$$B_{69} = -\frac{\partial I_{66}}{\partial q_5} = -2\left(m_5 r_5^2 + m_6 l_5^2\right)\sin q_5 \cos q_5$$

$$B_{60} = -2c_6 l_5 \sin q_5 \cos q_7 \cos(q_8 - q_6)$$

$$B_{7j} = -\frac{\partial I_{7j}}{\partial q_j} = c_6 l_j \cos q_j \cos q_7 \cos q_8, \quad j = 1,3,4$$

$$B_{72} = -c_6 l_2 \cos q_2 \cos q_7 \cos q_8$$

$$B_{75} = -\frac{\partial I_{75}}{\partial q_5} = c_6 l_5 (\sin q_5 \cos q_7 \cos(q_8 - q_6) - \cos q_5 \sin q_7),$$

$$B_{76} = c_6 l_5 \sin q_5 \cos q_7 \cos(q_8 - q_6),$$

$$B_{78} = m_6 r_6^2 \sin q_7 \cos q_7,$$

$$B_{79} = -\left(\frac{\partial I_{75}}{\partial q_6} + \frac{\partial I_{76}}{\partial q_5}\right) = 2c_6 l_5 \cos q_5 \cos q_7 \sin(q_6 - q_8),$$

$$B_{8j} = -\frac{\partial I_{8j}}{\partial q_j} = -c_6 l_j \cos q_j \sin q_7 \sin q_8, \quad j = 1,3,4$$

$$B_{82} = c_6 l_2 \cos q_2 \sin q_7 \sin q_8$$

$$B_{85} = B_{86} = c_6 l_5 \sin q_5 \sin q_7 \sin(q_6 - q_8),$$

$$B_{89} = -2c_6 l_5 \cos q_5 \sin q_7 \cos(q_6 - q_8).$$

The gravitational (8 × 1) matrix is

$$C(q) = \begin{bmatrix} -(m_1 r_1 + m_2 l_1) g \cos q_1 \\ m_2 r_2 g \cos q_2 \\ -(m_3 r_3 + (m_4 + m_5 + m_6) l_3) g \cos q_3 \\ -(m_4 r_4 + (m_5 + m_6) l_4) g \cos q_4 \\ -(m_5 r_5 + m_6 l_5) g \sin q_5 \\ 0 \\ -m_6 r_6 g \sin q_7 \\ 0 \end{bmatrix}.$$